Magnetic fields in close binary systems

Yu.N. Gnedin, T.M. Natsvlishvili

Central Astronomical Observatory at Pulkovo, St.Petersburg, Russia

Abstract.

We present a review of methods of measurements of stellar magnetic fields and current status of observational situation with magnetic field strengths for various types stars, presumably, for close binaries.

Direct methods of magnetic field measurements include: (a) Zeeman splitting of atomic lines, (b) circular spectropolarimetry, (c) broad-band circular polarimetry, (d) cyclotron spectroscopy.

Indirect methods include (a) Faraday rotation and spectrum of linear polarization, (b) effects of stellar activity, namely, the surface fluxes of chromospheric emission lines: Ca II H+K, Mg II H+K , Si II λ 1812 Å multiplet, C IV and X-ray fluxes versus B-V colours and luminosity classes, Rossby number and, especially, versus the mean magnetic flux density $< fB >$, (c) thermal and nonthermal radio emissions: gyroresonance and gyrosynchrotron emissions, plasma radiation, cyclotron maser, etc. We present the survey of the broad-band circular polarization measurements of Cataclysmic Variables (CVs) and of the radio continuum emission of RS Canum Venaticorum and related active binary systems.

Finally the last Table shows all current results of measurements of magnetic fields for various types of stars by direct and indirect methods.

1 Direct methods of stellar magnetic field measurements

One of the research areas which has recently shown a great growth is the study of stellar magnetic fields. The central direct method of measurement of stellar magnetic fields is based on the famous Zeeman effect of atomic spectral lines. There are the various cases of the Zeeman effect. The classical Zeeman splitting of atomic spectral lines is the usual situation for small and moderate magnetic field strength: $B \leq 10^3$ G, when the Coulomb energy is much stronger than the spin-orbit interaction and magnetic energies. The first intermediate regime occurs when the magnetic interactions are comparable to the spin-orbit interaction, both being small compared with Coulomb interaction.

The Paschen-Back effect occurs when the magnetic interactions are large compared to the spin-orbit interaction. As a result the magnetic interactions break the spin-orbit coupling. The typical values of magnetic field which produce the Paschen-Back effect are $B > 10^4$ G. When the magnetic field becomes very large $B \sim 10^5 \div 10^6$ G, it gives rise to the so-called quadratic Zeeman effect. In this case energy level splitting is proportional to the square of B (see for example, Dolginov et al., 1995):

$$(\Delta E)_B \approx e^2 B^2 a_0^2 n^4 (1 + m_e^2)/8 m_e c^2 = 0.616 \cdot 10^{-18} B^2 n^4 (1 + m_e^2), \tag{1}$$

where $a_0 = \hbar^2 / m_e e^2$ is the Bohr radius, n is the main quantum number and m^l is the orbital angular momentum projection on the magnetic field direction.

For wavelength displacement Eq (1) means

$$\Delta\lambda \sim \lambda^2 n^4 B^2. \tag{2}$$

Finally, for magnetic field magnitudes $B \sim (10^7 \div 10^8)$ G the magnetic interactions are comparable to the Coulomb interaction. This region is difficult to study, and numerical techniques have been usually used.

Atomic structure is affected by strong magnetic fields. The critical value of the field at which the essential reform of an atom becomes important is determined by comparing the cyclotron energy $\hbar\omega_B \equiv \hbar eB/m_e c$ with the Rydberg energy:

$$E_0 = Z^2 e^4 m_e / 2\hbar^2 \approx 13.6 Z^2 eV \tag{3}$$

which is typical of the Coulomb binding. A magnetic field will be termed superstrong if $\hbar\omega_B > E_0$; this implies a field strength

$$B \geq B_0 = 2Z^2 m_e^2 e^3 c/\hbar^2 = 4.7Z^2 \cdot 10^9 \mathrm{G} \tag{4}$$

By convention, B^0 is chosen in such a way that $\hbar\omega_B = 4E_0$.

If $B \gg B^0$, the magnetic forces acting on an atomic electron dominate over the Coulomb forces, the transverse size of the atom becoming smaller than the Bohr radius and the transverse velocity of the electron becoming greater than the longitudinal one.

The next very important direct method of magnetic field measurement is circular polarimetry of wings of atomic lines (circular spectropolarimetry). The degree of circular polarization P_v is determined by the gradient of intensity $I_{(\lambda)}$ in the line wing (see Schmidt et al., 1992):

$$P_v(\%) = \frac{1.1}{I(\lambda)} \frac{dI}{d\lambda} B_s \left(\frac{\lambda}{4861\text{Å}} \right)^2, \tag{5}$$

where B^s is the magnetic field strength in kG, λ - the wavelength in Angstroms. Net polarization of 0.1% in the wing of H_β line corresponds to a magnetic field magnitude of $B^s \cong 10$ kG.

The next effective direct method of magnetic field measurement is broad-band polarimetry of continuum radiation. The incident onto plasma with a magnetic field electromagnetic wave produces oscillations of an electron velocity. As a result an additional Lorentz force appears

$$F_{tot} = F\left(\frac{\omega_B}{\omega} \overline{B} {}^\wedge \overline{E} \right), \tag{6}$$

which depends on the ratio of the cyclotron frequency $\omega_B = eB/m^e c = 1.76 \cdot 10^7 B$ to radiation frequency and on the angle between the directions of the electromagnetic vector E and of the magnetic field B. As a result of action of this Lorentz force magnetized plasma acquires dichroizm and birefregence properties, becoming similar to any anisotropic medium. In an anisotropic medium two types of electromagnetic waves (normal modes or normal waves) should be propagated (see Fig.l). These normal waves are usually called as ordinary (O.W.) and extraordinary waves (E.O.W.) with their intrinsic refraction indices, phase velocities and polarizations. O.W. behaves as a usual electromagnetic wave in a plasma without a magnetic field. For E.O.W. transport coefficients for various emission (magnetobremsstrahlung) and scattering (electron scattering) processes have a resonance at cyclotron frequency ω_B.

In consequence the magnetized plasma radiation becomes strongly polarized, character and degree of polarization depending on the radiation frequency and the angle between radiation and magnetic field directions. The radiation directed along the magnetic field acquires only the circular polarization

$$\Theta = 0, \pi, \quad P_v \neq 0, \quad P_e = 0. \tag{7}$$

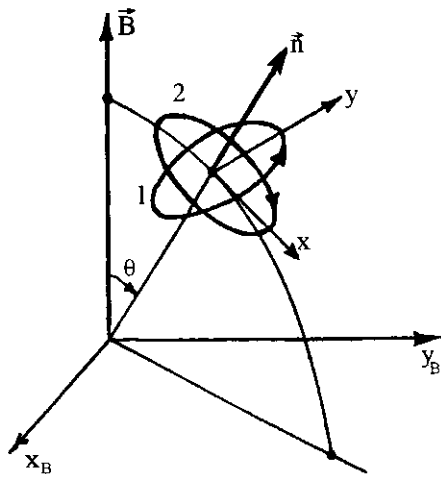

Figure 1: Polarization ellipses for normal modes: (1) extraordinary wave (E.O.W.), (2) ordinary wave (O.W.)

For transverse propagation the radiation of a plasma with a magnetic field is linearly polarized:

$$\Theta = \pi/2, \quad P_v = 0, \quad P_e = 0. \tag{8}$$

For $\Theta \neq 0, \pi/2$ or π the radiation is polarized elliptically.

In the case when the radiation frequency ω is much larger than the cyclotron frequency ω_B, the radiation is predominantly circularly polarized:

$$\omega \gg \omega_B, \quad P_v \sim (\omega_B/\omega)\cos\Theta, \quad P_e \sim P_v^2 \sim (\omega_B/\omega)^2. \tag{9}$$

Practically the following expression can be used to estimate magnetic field:

$$P_v \sim (\omega_B/\omega) \cong 10^{-8}\lambda(\mu)B(\mathrm{G}) \sim 0.1\%(B/10\mathrm{G})(\lambda/1cm). \tag{10}$$

In the opposite case $\omega \gg \omega_B$ the radiation of a plasma is predominantly linearly polarized:

$$\omega_B \gg \omega, \quad P_e \sim 1 \gg P_v \sim \omega/\omega_B. \tag{11}$$

The most important case is the cyclotron resonance: $\omega \sim \omega_B$. For the optical range this case corresponds to magnetic field strengths: $B \sim 10^7 \div 10^8$ G. At cyclotron resonance the plasma radiation is completely polarized:

$$P_e = \sin^2\Theta/(1+\cos^2\Theta), \quad P_v = 2\cos\Theta/(1+\cos^2\Theta), \quad P_e^2 + P_v^2 = 1. \tag{12}$$

It means that the cyclotron radiation at the first harmonic is completely elliptically polarized.

A very effective method of measurement of magnetic field of compact stars (white dwarfs, for instance) is to use the ratio of two Stokes parameters:

$$Q/V = 1/2(\omega_B/\omega)(\sin^2\Theta/\cos\Theta). \tag{13}$$

One can see that the methods presented here allow one to measure magnetic field of stellar objects directly without using any model consideration.

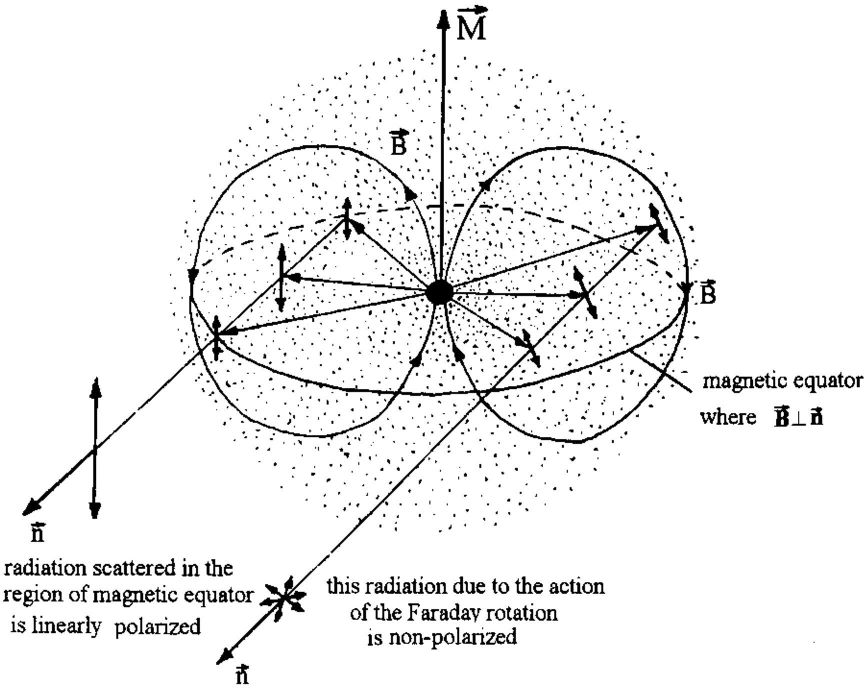

Figure 2: Faraday rotation phenomenon in spherically symmetric circumstellar envelope of a hot star with the dipole magnetic field.

2 Indirect methods of determination of magnetic fields

One of these methods has been recently developed by Gnedin and Silant'ev, (1980; 1984). Thompson scattering by electrons gives an important contribution to generation process of intrinsic polarization of hot stars and circumstellar shells. It is well known that optical radiation from Be stars is observed to be intrinsically linearly polarized. The main reason of this polarization is the asymmetric disk-like shape of the circumstellar envelope.

If there is a magnetic field at the surface of a star, then, even if the latter is spherically symmetric, the radiation from it will possess integral intrinsic linear polarization.

Many hot stars have the envelopes consisting of magnetized plasma. The radiation of such stars acquires linear polarization as a result of single scattering on electrons in the envelopes. This scattered radiation undergoes Faraday rotation by propagation in the magnetized plasma of the envelope. The angle of the Faraday rotation χ is determined by the expression:

$$\chi = \frac{1}{2}\psi_V = \frac{1}{2}\tau_T\delta\cos\Theta \cong 0.8\lambda^2(\mu)B(G)\tau_T\cos\Theta. \tag{14}$$

The existing magnetic field of the envelope is an additional factor of optical anisotropy. According to the general geometrical arguments discussed above the integral linear polarization of light will exist even for a spherically symmetric envelope if the magnetic field has no axial symmetry about the line of sight. To understand in more detail the mechanism of this effect, let us consider a spherical envelope with a magnetic dipole. We assume also that the magnetic dipole M is perpendicular to the line of sigth n (see Fig.2).

For small magnetic fields (or small wave lengths) the Faraday rotation effect is negligible ($\chi \ll 1$)

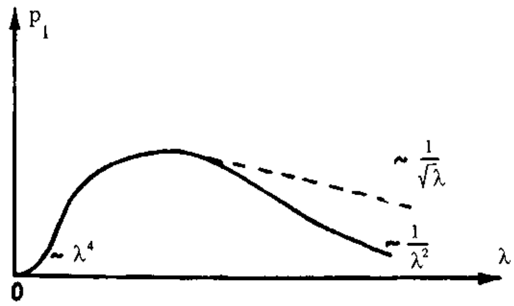

Figure 3: The spectrum of linear polarization for a spherical circumstellar envelope of a hot star with the dipole magnetic field.

and the integral polarization from a spherical envelope is equal to zero because of axial symmetry of the scattering picture. With increasing magnetic field the angle χ increases too, and, the partly polarized scattered radiation begins to undergo Faraday rotation. The rotation angles χ are different for the waves scattered in different volumes along the line of sight n, and, as a result, the total radiation, from all volume elements, will be depolarized (see Fig.2). But in the magnetic equator volumes Faraday rotation practically does not occur ($\cos\Theta \cong 0$ and $\chi \cong 0$). The radiation scattered in the equatorial volumes is partly polarized in the plane *(nM)* and it is this radiation that gives rise to a nonzero integral polarization from the magnetized envelope. The increase in magnetic field (or increase in wavelengths) decreases the width of the equatorial region with $\chi \ll 1$, and the amount of linearly polarized radiation from this region begins to decrease. So, the maximum integral polarization corresponds to such magnetic fields and wavelengths when the mean rotation angle $\chi \cong 1$.

The qualitative form of the spectrum of the integral linear polarization $p_l(\lambda)$ is presented in Fig.3. The decrease of polarization for large wavelengths, corresponding to $\chi \gg 1$, depends on the form of electron distribution in the envelope. If the density number $N_e(r)$ in the envelope is constant then $p_l \propto \lambda^{-2}$. For the case $N_e \propto r^{-2}$ one has $p_l \propto \lambda^{-1/2}$.

Fig.4 shows the spectrum of linear polarization for a case of magnetized stellar wind. One can see the difference in the spectra in Figs. 3 and 4. It means that this method allows one to distinguish between the various cases of magnetic field geometry.

The Faraday rotation method has been applied to T Tau (Gnedin and Red'kina, 1984; Gnedin et al., 1988) and Herbig Ae/Be stars (Gnedin and Pogodin, 1985; Pogodin, 1992; Beskrovnaya and Pogodin, this volume).

Let us turn to the consideration of various types of stellar activity as methods of estimation of magnetic field magnitudes. The first rough estimation can be made using simple equipartition relation. Fig.5, taken from Vilhu (1986) shows the equipartition magnetic field strength $B_{eq} = (8\pi\, p_{GAS}(\tau = 1))^{1/2}$ plotted versus the observed magnetic field strength. This result has been confirmed by Saar and Linsky (1985) observations mostly of G and K dwarfs. They have discovered that B increases with descreasing T_e in a manner consistent with $B \sim P_{gas}^{1/2}$, suggesting equipartition between the magnetic and gas pressures in the photosphere of stars.

Marcy (1984) showed a correlation between the magnetic flux, Ca II flux and X-ray luminosity L_x. To study the magnetic field activity relations Saar et al. (1987) have compared photosphere magnetic flux densities, i.e. the product $< f\ B >$, where f is the fillfactor, with the observed outer atmosphere emission. Fig.6 shows Ca II H+K excess flux density F_{CaII} versus $< fB >$. Fig.7 shows the soft X-ray flux density F_x versus the mean magnetic flux density $< fB >$. The Ca II H+K

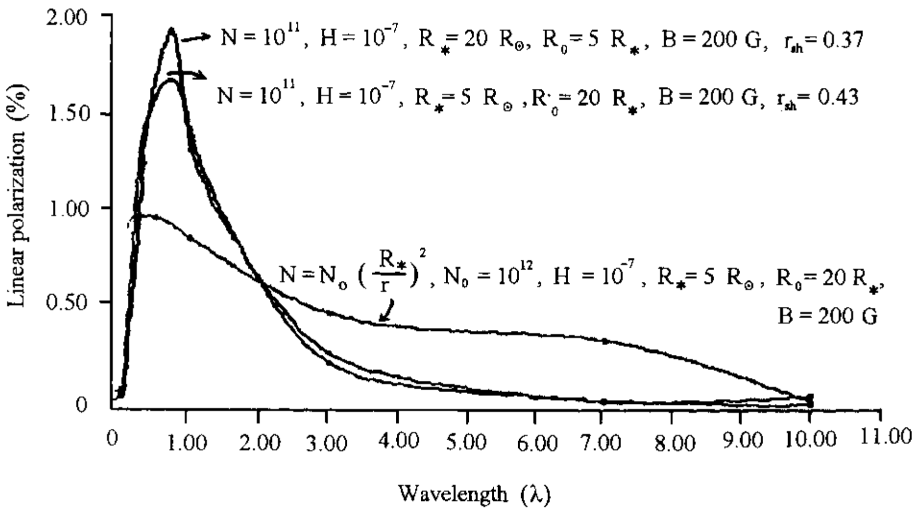

Figure 4: The same as Fig.3 only for the case of magnetized stellar wind.

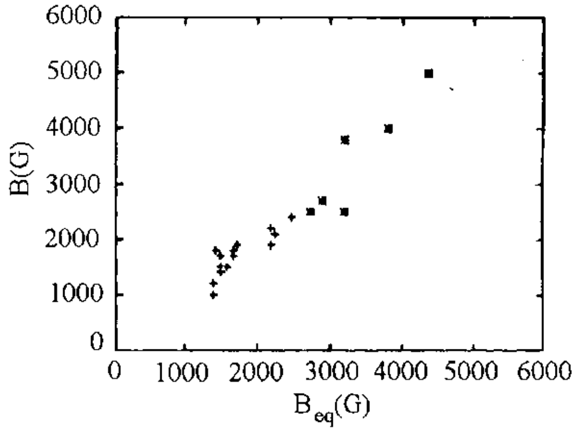

Figure 5: The dependence of observed magnetic field strength on the equipartition magnetic field, taken from Vilhu (1986).

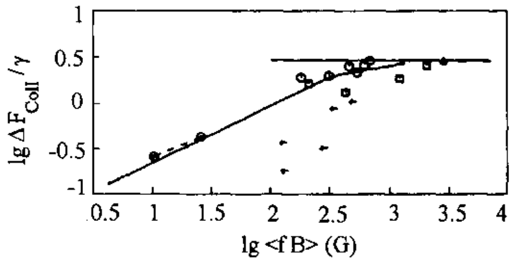

Figure 6: Ca II H+K excess flux density versus $< fB >$ (Schrijver et al., 1988).

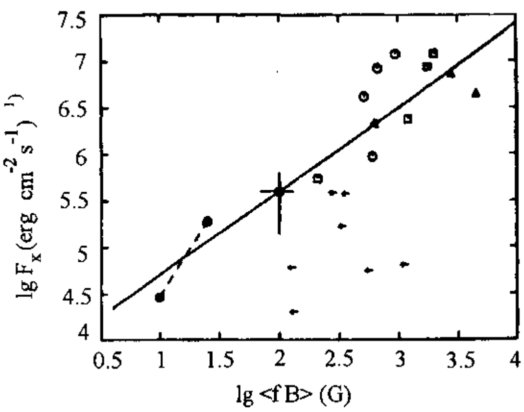

Figure 7: The soft X-ray flux versus $< fB >$ (Schrijver et al., 1988).

excess flux density appears to saturate for values of $< fB >$ over 300 G. No such saturation is seen in F_x versus $< fB >$. The power law of Fig.6 fits (Schrijver et al., 1988):

$$\Delta F_{CaII} = 0.055 < fB >^{0.62} . \tag{15}$$

Using the observational data of Figs. 6 and 7, it is possible to fit the mean magnetic flux density to the following expression (Skumanich et al., 1975):

$$< fB >= 2800R_c - 200\mathrm{G}, \tag{16}$$

where R_c is the intensity of the Ca II H+K flux.

Finally, the observation thermal and nonthermal radio emission of stars allows us to determine stellar magnetc fields. The principal mechanisms of radio emission depending on magnetic field are: gyroresonance and gyrosynchrotron emissions, plasma and cyclotron maser radiations (see in detail below).

3 Circular polarization of cataclysmic variables: AM Her type CVs, intermediate polars

An AM Her-type mass-transfer binary displays strong circular polarization in its optical flux, caused by high harmonic cyclotron emission from the vicinity of the accretion shock (Stockman et

Table 1: CVs exhibiting circular polarization

Object	Period(min)	P_v^{max}/B
RE 1307+535	79.7	50%
EF Eri	81.0	$20\%/10^8$
DP Leo	89.8	$35\%/5\cdot10^7$
VV Pup	100.4	$15\%/3\cdot10^7$
V834 Cen	101.5	19%
H1907+690	104.6	
Grus V1	108.6	
MR Ser	113.6	$12\%/2.6\cdot10^7$
BL Hyi	113.6	$15\%/4\cdot10^7$
ST Leo	113.9	$20\%/3.2\cdot10^7$
EK UMa	114.5	
WW Hor	114.6	$5.5\cdot10^7$
AN UMa	114.8	$35\%/10^8$
UZ For	126.5	
M Her	185.6	$10\%/2\cdot10^7$
BG CMi	194.4	1%*Asynchr*
BY Cam	198	*Asynchr*
V 1500 Cyg	201.0	*Asynchr*
QQ Vul	222.5	7.5%
EXO 032957-2606.9	228.0	$10\%/5.5\cdot10^7$

al., 1992). Circular polarization is the best direct evidence for magnetic field white dwarf primaries in these CVs, indicating high field strengths of $B \geq 10^7$ G. 19 polarized, high-field CV systems (Table 1) are well-known now.

Lack of AM Her variables with fields stronger than have been observed $(B > 10^8$ G) and asynchronous CV systems with moderate fields $(B > 5 \cdot 10^6$ G) is not due to selection effects or to the survey sensitivity but must represent difference in the period evolution of magnetic systems with respect to nonmagnetic CVs. Stockman et al. (1992) suggest that asynchronous diskless magnetic CVs may accelerate their evolution through "propeller-like" expulsion of material and associated angular momentum.

In an AM Her accretion binary the magnetic field prevents the formation of a normal accretion disk and, through its interaction with the secondary star, synchronizes the white dwarf rotation with the orbital period (80 min$< P <$ 4 hr).

For more than 75 selected CVs and X-ray binaries Stockman et al. (1992) have obtained integrated broadband polarizations in both optical and infrared bands.

67 CVs and X-ray binaries are observed to have negligible circular polarization. Synchronous or nearly synchronous AM Her systems listed in Table 1 comprise 10% of all CVs and over 16% of all CVs with periods less than 4 hr.

In the Ritter (1990) catalog of CVs with known periods there are 11 systems with coherent X-ray or optical periods significantly shorter than their orbital (spectroscopic) periods — Intermediate Polars (IP).

If the AM Her systems have higher magnetic fields and magnetic moments than IPs, why do we not find asynchronous systems with intermediate magnetic moments and with periods between 3 and 5 hr? Except for EX Hya, why do we not find IPs with $P_{orb} < 2$ hr? The evolutionary models attempted to explain lack of short-period IPs. Lack of long-period IPs with detectable optical polarization is also problematic. Several authors have concluded that such systems will accrete directly from the accretion stream, being unable to form even a truncated accretion disk, argue that diskless IP systems may accrete by blobs rather than a diffuse accretion stream.

Alternatively, Stockman et al. (1992) suggest that diskless accretion may significantly affect stability and evolution of IPs and may explain relative lack of such systems, particularly at shorter periods. White dwarfs in such systems do not offset the accretion torques through magnetic interactions with a surrounding accretion disk or a secondary star. Instead, the incoming stream is accreted directly or forms a ring of orbiting material. Therefore, it seems unlikely that offsetting torques can be obtained by magnetic interactions with the incoming accretion stream for the lower field strengths or higher accretion rates expected in diskless IPs. Depending on the spin period of the white dwarf, much of orbiting, nonvisions ring will be threaded and expelled from the system as a magnetic wind rather than be accreted.

Direct accretion from the accretion stream by separate blobs takes place rather than a diffuse accretion stream (King and Lasota, 1991). In this case the accretion power would emerge in the unseen EUV and soft X-ray band to provide $L_{sx} \gg L_{hx} \leq L_{opt}$.

There is another mechanism which provides the outflow of the matter and angular momentum loss. The outflow of the matter in the vicinity of the magnetic WD poles would be produced due to the cyclotron resonance radiation pressure (Voykhanskaya and Gnedin, 1991). Mitrofanov and Pavlov (1982) have drawn attention to the fact that the radiative force on electrons increases in a strong magnetic field. This increase is due to a resonance in the electron scattering cross-section at the cyclotron frequency $\omega_B = eB/m_e c$.

$$\sigma_{E.W.} = \sigma_T \omega/(\omega - \omega_B)^2, \quad \sigma_{O.W.} \approx \sigma_T. \tag{17}$$

For the cyclotron frequency lying in the optical spectral range the resonance magnetic field strength corresponds to

$$B_{res} = 3.6 \cdot 10^{-7} \nu \cong (8 \cdot 10^7 \div 3 \cdot 10^9) G. \tag{18}$$

This mechanism may be probably a reason for lack of AM Her systems with higher field strengths. One should expect, as evidence of magnetic wind or cyclotron resonance outflow, distortion of radial velocity curves, Balmer decrement and the X-ray flux variations (Voykhanskaya and Gnedin, 1991). Bespalov and Zheleznyakov (1990) have developed a model of a radiative discon. It means a model of a plasma envelope of a hot magnetic WD with high radiation pressure due to cyclotron resonance (Fig.**8**).

The angular momentum loss processes can be associated with the following turbulent mechanisms:

(a) MHD-driven winds from accretion disks (Cannizo and Pudritz, 1988);

(b) nonlinear three-mode coupling processes in plasma turbulence including three-wave resonance, nonlinear Landau resonance and plasma-maser instability (Nambu and Hada, 1993).

In conclusion of this Section we would like to mention up-to-date record minimal circular polarization data. Kemp et al. (1985) have detected circular polarization of λ and RS CVn star at the level

$$P_v = (0.002 \div 0.004)\%.$$

Nadeau and Bastien (1986) have detected circular polarization of a few T Tau stars with extremely high accuracy:

$$RY\ Tau : P_v = 5 \cdot 10^{-5}, \quad T\ Tau : P_v = 2 \cdot 10^{-5},$$

$$SU\ Aur : P_v = 4 \cdot 10^{-6}, \quad DG\ Tau : P_v = 10^{-4},$$

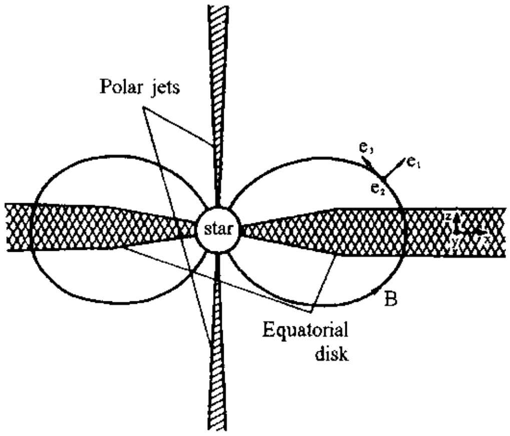

Figure 8: Discon: plasma envelope of a hot magnetic WD with high radiation pressure due to cyclotron resonance, from Bespalov and Zheleznyakov (1990).

$$FU\ Ori : P_v = 2 \cdot 10^{-5}.$$

These extremely small polarization degrees correspond to magnetic field values $B \leq 10^3$G.

4 Radio continuum emission of RS Canum Venaticorum and related active binary systems

It has been discovered that only a small fraction of ordinary stars are comparatively luminous in the radio though the fraction of the total energy emitted in the radio is small. Stars detectable in the radio because of thermal processes must have large effective emitting surfaces resulting from the presence of strong mass outflows. Stars are also detectable if nonthermal processes ensure a high effective brightness at the radio wavelengths. Fig.9 represents the detected radioflux level from stars of various types.

The detection of radio emission from close binaries can be due to the influence of a stellar companion. Table 2 shows the results of Drake et al. (1986) survey of nonthermal radio emission of active binary systems. Typical value of spectral fluxes lies in the range log F(erg/Hz) = 15 - 16.5. In the last survey (Drake et al., 1989; 1992) 122 RS CVn stars were observed, 66 of which were detected on one or more occasions. The limit of the radioflux at the 6 cm wavelength is 0.2 mJy.

From the observations one easily derives correlations of radio properties of stellar systems with various systematic and stellar parameters: P_{orb}, P_{rot}, V_{rot}, CIV, X-ray emissions, etc.:

$$F_G \sim V_{rot}^{1.0\pm0.3}, \quad F_G/F_{bol} \sim P_{orb}^{-0.9\pm0.2} \sim V_{rot}^{1.4\pm0.3}.$$

Active dwarf binaries as a rule exhibit no statistically significant correlation. Active subgiant and giant binaries do show a significant correlation:

$$L_G/L_{bol} \sim P_{rot}^{-1.1} \sim V_{rot}^{-1}.$$

This would imply that the binarity does not directly control the extent of their radio emissions but rather that it is their rapid rotation.

$$L_G/L_{bol} \sim (L_X/L_{bol})^{1.4\pm0.1} \sim (L_{CIV}/L_{bol})^{2.2\pm0.3}.$$

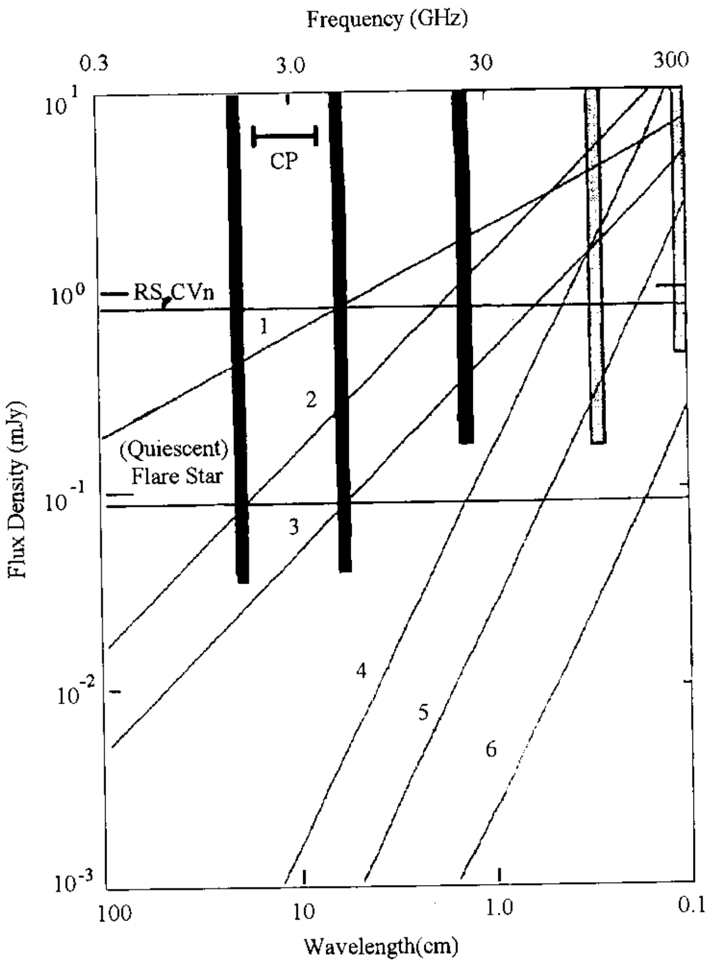

ure 9: Radioflux level detected from stars of various types (Sequist, 1996). 1 – symbiotic, WR & ; 2 – red supergiant; 3 – red giant; 4 – MO supergiant (photosphere); 5 – MO giant (photosphere); Sun (photosphere).

Table 2: Nonthermal radio emission of active binary systems (RS Canum Venaticorum, Drake et al. (1986)).

System	Spectral Type	P_{orb}	V	$F_6(mJy)$	D(pc)
XY UMa	G2-5V+K5V	$0^d.479$	$9^m.8$	0.3 ± 0.1	100
HD 8358	G5V+G5V	$0^d.516$	$8^m.25$	2.72 ± 0.06	65
ER Vul	G0V+G5V	$0^d.698$	$7^m.27$	4.97 ± 0.11	45
UV Psc	G2IV-V+K0IV	$0^d.861$	$9^m.1$	0.89 ± 0.05	165
V772Her	G0V+M0V	$0^d.879$	$7^m.07$	0.98 ± 0.08	42
DH Leo	K0V+	$1^d.070$	$7^m.8$	0.77 ± 0.07	30
RZ Cas (Algol)	A2V+G6IV	$1^d.195$	$6^m.35$	1.36 ± 0.06	75
HD166181	G5V+dM	$1^d.810$	$7^m.66$	1.56 ± 0.1	36

Table 2 allows us to estimate the magnetic field strength and electron density of the extended halo region in which thermal gyrosynchrotron emission is actually produced:

$$N_e \approx 2 \cdot 10^8 cm^{-3},\ B \approx 200\text{G}.$$

Table 3 represents basic radio emission mechanisms which are responsible for radio emission of stars.

5 Radio emission from CP stars (Seaquist, 1996)

These chemically peculiar stars are expected to exhibit nonthermal radio emission because of the existence of strong magnetic fields. Using the VLA Drake et al. (1987) detected 5 from the sample of 33 CP stars, namely, σ Ori E and the famous "Babcock's Star" GL Lac (=HD 215441).

More than 60 stars have been searched for, which resulted in 16 detections at 6 cm, with the highest detection rate in the He-S category. None of the Ap stars with Sr-Cr-Eu abundance anomalies have been detected to date. One of the detected stars is a magnetic B star in the ρ Oph cloud and is embedded in a diffuse shell of ionized hydrogen meaning that it must be a very young object. Overall range of luminosity for the detected objects is $L^G = (10^{16.8} \div 10^{17.9})$ erg/sHz. The general radio characteristics, such as a flat radio spectrum ($F_\nu \sim \nu^{-\alpha}$, $\alpha \sim 0$), measurable circular polarization and nonthermal brightness temperatures are consistent with gyrosynchrotron emission (see Tabl. 3).

Linsky et al. (1992) suggest CP stars to be a distinct class of radio emitters neither like the stars with stellar winds nor the stars with solar-type magnetic activity. VLBI observations indicate that the radio emission occurs in a compact region within a few stellar radii. One can probably consider these regions as radiation belts where accelerated particles are captured by magnetic field lines. Alternative model suggested by Leone (1991) considers radio emission as gyroresonance emission from thermal electrons in wind escaping from the magnetic poles. Further development of theory is required to explain the phenomenon of radio emission of magnetic CP stars.

6 Conclusions

In the last Section of our review we present the current status of observed magnetism of various type stars. Table 4 shows type of star (first column), directly measured or indirectly estimated stellar magnetic field magnitude (second column), and radiation mechanism or method of measurement (third column).

Table 3: Radio emission mechanisms

Mechanisms	Sourse size	T_B	Circul. polar.	Time Var.	Stars where observed
Thermal bremsstrahlung	large $R \gg R_s$	low $\sim 10^4$	low (~ 0)	low (years)	Sun, OB stars, K, M giants
Gyroresonance emission	large $R > R_s$	10^7	low	low	Sun, AM Her quiescent comp αM_e
Gyrosynchrotron or synchrotron	moderate $R \leq R_s$	$10^8 - 10^{10}$	mod. $< 30\%$	mod. (min,hr)	Sun, αM_e, RS CVn OB, B_P, A_P(CP)
Cyclotron maser	small $R \ll R_s$	high 10^{20}	$\sim 100\%$	high	Sun, αM_E flare AM Her-outburst
Plasma radiation+plasma-maser instability	small $R \ll R_s$	10^{17}	$(10 \div 90)\%$	high	Sun, αM_E flare, AM Her-outburst

Nonlinear wave processes: plasma–maser instability between low frequency modes and high–frequency electron cyclotron mode:
a) lower–hybrid resonance modes: T_{11} increases by a factor ~ 10;
b) ion cyclotron modes amplify electr. Cyclotron EX mode;
c) Langmuir turbulence amplify both EX and O modes — no polarization.

Acknowledgements. The preparation of this review was supported by grants from Russian Foundation of Basic Research and Program "Astronomy-96" from Russian Ministry of Science and from INTAS.

References

Beskrovnaya N.G., Pogodin M.A.: 1996, this volume.

Bespalov P.A., Zheleznyakov V.V.: 1990, Sov.Astron.Lett., 16, 442.

Cannizo J.K., Pudritz R.E.: 1988, Astrophys. J., 327, 840.

Dolginov A.Z., Gnedin Yu.N., Silant'ev N.A.: 1995, Propagation and Polarization of Radiation in Cosmic Media, Gordon and Breach Publishers.

Linsky J.L.: 1987, Astrophys. J., 332, 902.

Drake S.A., Simon T., Linsky J.E.: 1986, Astron. J., 91, 1229.

Drake S.A., Simon T., Linsky J.E.: 1989, Astrophys. J. Suppl. Ser., 71, 905.

Drake S.A., Simon T., Linsky J.E.: 1992, Astrophys. J. Suppl. Ser., 82, 311.

Gnedin Yu.N., Pogodin M.A.: 1985, Sov. Astron. Lett., 11, 18.

Gnedin Yu.N., Red'kina N.P.: 1984, Sov.Astron. Lett., 10, 255.

Gnedin Yu.N., Red'kina N.P., Tarasov K.V.: 1988, Sov. Astron., 32, 186.

Gnedin Yu.N., Silant'ev N.A.: 1980, Sov. Astron. Lett., 6, 190.

Gnedin Yu.N., Silant'ev N.A.: 1984, Astrophys. Space Sci., 102, 375.

Johns-Krull Ch.M., Valenti J.A.: 1996, Astrophys. J. Lett., 450, L95.

Kemp J.C, Henson G.D., Krauss D.J., Dunaway M.K.: 1985, Bull. Amer. Astron. Soc, 19, 752.

King A.P., Lasota J.-P.: 1991, Astrophys. J., 378, 364.

Leone F.: 1991, Astron. Astrophys., 252, 198.

Linsky J.L., Drake S.A., Bastien T.S.: 1992, Astrophys. J., 393, 341.

Maheswarand M., Cassinelli J.P.: 1988, Astrophys. J., 335, 931.

Table 4:

Type of star	Magnetic field magnitude	Radiation mechanism or measurement method
Neutron stars (Radiopulsars)	$(10^{12} \div 10^{13})$Gs for Her X-1 5×10^{12}G($\sim 10^{12}$G)	Cyclotron lines in X-ray (Radioemission pattern) $L \sim B_s^2 R_s^6 \Omega^4$
White dwarfs	$(10^6 \div 10^8)$G	Circular polarimetry Zeeman splitting in a strong magnetic field
Magnetic Ap stars	$(10^3 \div 10^4)$G	Zeeman splitting
RS Canum Venaticorum Expanded halo	$\sim 10^3$G ~ 200G	High resolution spectrum Circular polarimetry (Kemp et al., 1985) Thermal gyrosynchrotron
Flare stars	$\geq 10^3$G for AD Leonis (dM3.5e)3.5×10^3G	High resolution Infrared spectroscopy (Johns-Krull, Valenti, 1996)
WR stars Nonthermal radioemission W-R $\sim$1/6 of thermal ones or 1/3 OB stars	~ 1500G ~ 100G ~ 10G	Magnetic stellar wind (Maheswarand and Casinelly, 1988): $B_r(R) \leq M^{1/2}U^{3/2}/\Omega R^2)$ Gyroresonance radiation from the surface of hot stars (Underhill, 1994) Shock acceleration (White, 1985)
T Tau	$(10^3 \div 10^4)$G	Circular polarimetry (Nadeau and Bastien, 1986) Linear polarization with Faraday rotation (Gnedin and Red'kina, 1984)
Be stars	$(10 \div 100)$G	Magnetic stellar wind (Maheswarand and Cassinelli, 1988) Linear polarization with Faraday rotation (Gnedin and Silan'tev, 1984)
Early-type stars ($\xi Per, \lambda Cep$)	$(70 \div 200)$G	Magnetic stellar wind
Cool dwarfs, G dwarfs	$(20 \div 300)$G	Equipartition CaIIH+K Fluxes

Marcy G.M.: 1984, Astrophys. J., 276, 286.
Mitrofanov I.G., Pavlov G.G.: 1982, Mon. Not. R. Astron. Soc, 200, 1033.
Nadeau R., Bastien P.: 1986, Astrophys. J. Lett., 305, L5.
Nambu M., Hada T.: 1993, Phys. Fluids, 5, 742.
Pogodin M.A.: 1992, Sov. Astron. Lett., 18, 178.
Saar S.H., Linsky J.L.: 1985, Astrophys. J. Lett., 229, L47.
Schmidt G.D., Bergeron P., Liebert J., Saffer R.A.: 1992, Astrophys. J., 394, 603.
Schrijver C.J., Cote J., Zwaan C, Saar S.H.: 1988, Astrophys. J., 337, 964.
Seaquist E.R.: 1996, Rep. Progr. Phys., (in press).
Skumanich A., Smythe G., Frazier E.W.: 1975, Astrophys. J., 200, 747.
Stockman H.S., Schmidt G.D., Berriman G., Liebert J., Moore R.L., Wickramasinghe D.T.: 1992, Astrophys. J., 401, 628.
Ritter H.: 1990, Astron. Astrophys. Suppl. Ser., 85, 1179.
Underhill A.B.: 1984, Astrophys. J., 276, 583.
Vilhu O.: 1986, in: Swings J.P. (ed.), "Highlight of Astronomy", 467.
Voykhanskaya N.F., Gnedin Yu.N.: 1991, Astrofiz. Issled. (Izv. SAO), 33, 71.
White R.L.: 1985, Astrophys. J., 289, 698.